

Supporting Information for

Stereoelectronic interactions are too weak to explain the molecular conformation in solid state of *cis*-2-*tert*-butyl-5-(*tert*-butylsulfonyl)-1,3-dioxane

Fátima M. Soto-Suarez,^a Tania Rojo-Portillo,^a Eduardo Hernández-Huerta,^a Alejandro Aguilera-Cruz,^a Alberto Tapia-Bárcenas,^a David Atahualpa Contreras-Cruz,^a Rubén A. Toscano,^a Beatriz Quiróz-García;^a Aaron Rojas-Aguilar,^b Fernando Cortés-Guzmán,^a John Bacsa,^c Karla Ramírez-Gualito;^d José Enrique Barquera-Lozada,^a Gabriel Cuevas. ^{a*}

^a. Universidad Nacional Autónoma de México, Instituto de Química, Circuito Exterior, Ciudad Universitaria, Delegación Coyoacán, C.P.04510 Ciudad de México, México. E-mail: gecgb@unam.mx

^b. Departamento de Química, Centro de Investigación y de Estudios Avanzados del IPN, Av. Instituto Politécnico Nacional 2508, C.P. 072360, Ciudad de México, México.

^c. School of Chemistry and Biochemistry, Georgia Institute of Technology, Atlanta, Georgia 30332-0400, USA.

^d. Centro de Nanociencias Micro y Nanotecnologías. Instituto Politécnico Nacional. Luis Enrique Erro, s/n, Nueva Industrial Vallejo. Gustavo A Madero, 07738, Ciudad de México, México.

Table of Contents

Computational Data	S2
X ray determination.	S5
Topological theory of atoms in molecules section	S12
Thermochemistry section	S16
Determination of Enthalpies of Fusion	S17
Determination of Enthalpies of Sublimation	S18
References	S22

Computational Data

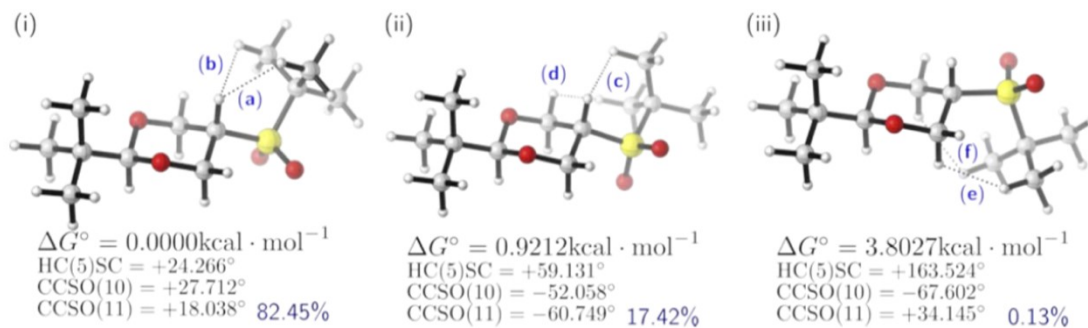


Figure S1. Relative energy of the stationary states of minima energy of *trans-1* at M06-2X/6-311++G(2d,2p) level of theory.

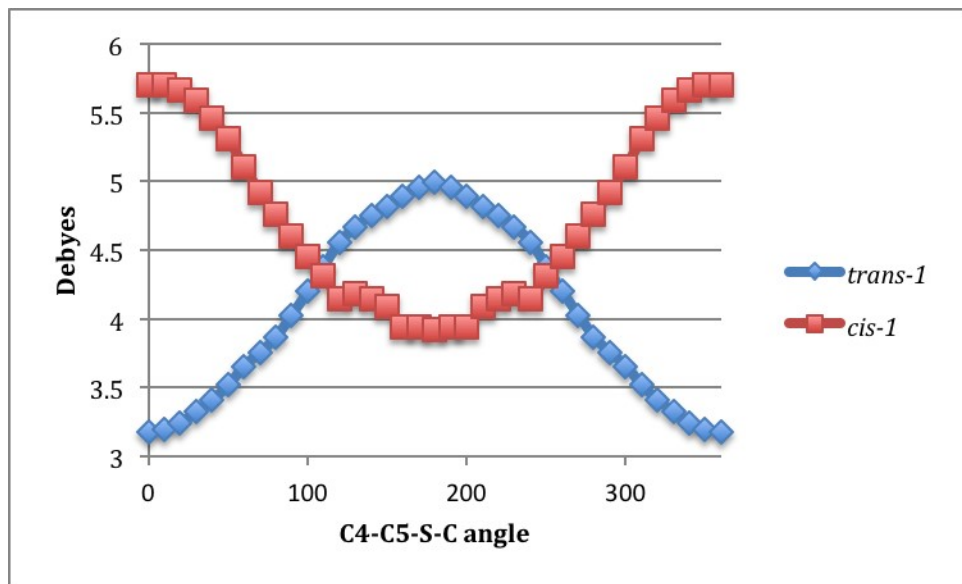


Figure S2 Evolution of the molecular moment (Debyes) as a function of the rotation of the C5-S bond for *cis* and *trans-1* at M06-2X/6-311++G(2d,2p).

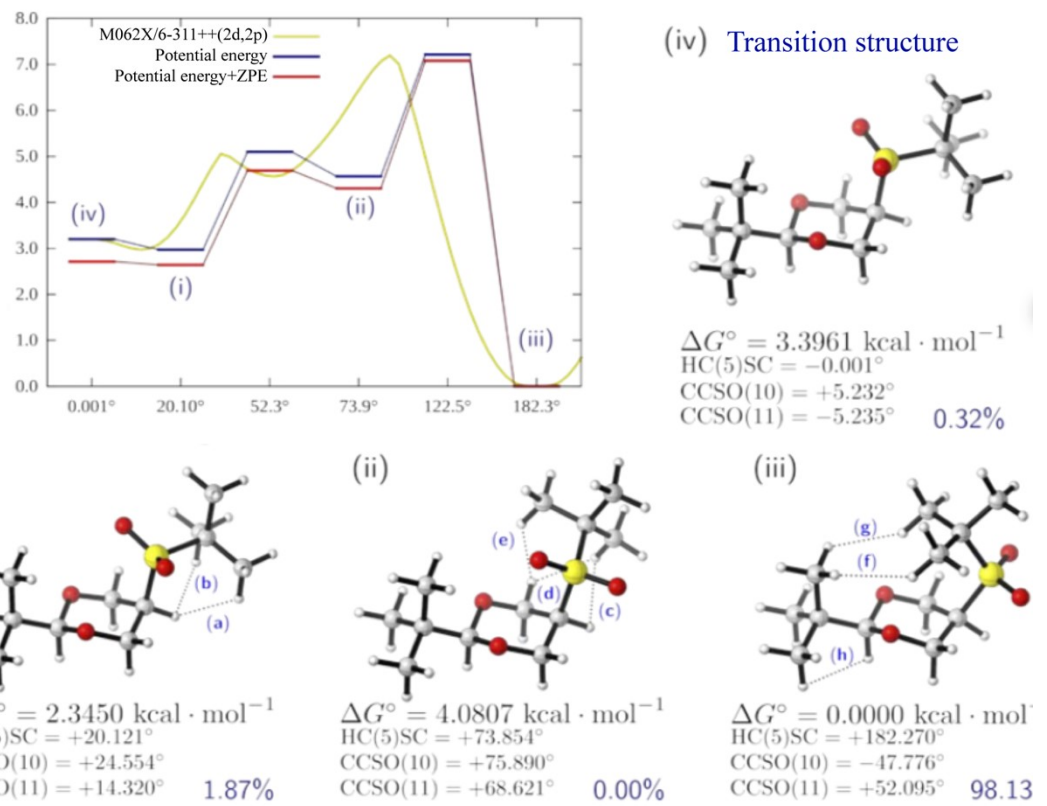


Figure S3 Stationary states related to the rotation of the C5-S bond in *cis*-1 at M06-2X/6-311++G(2d,2p) level of theory.

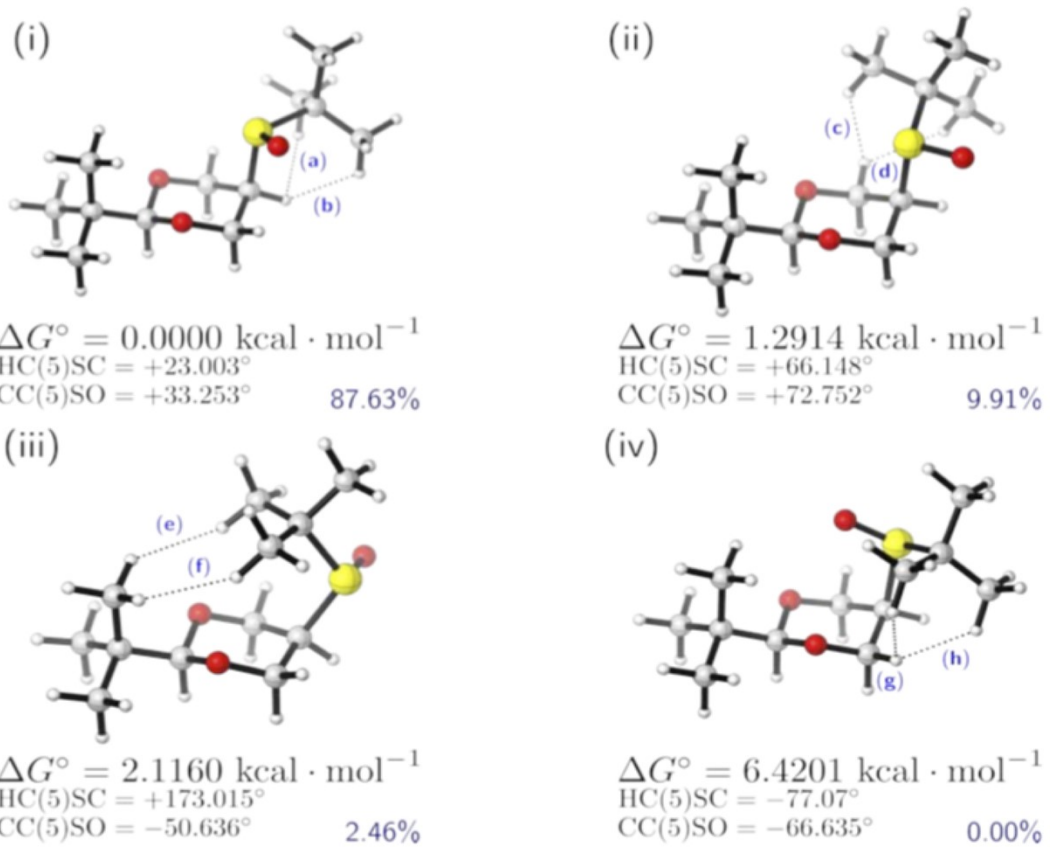


Figure S4 Stationary states related to the rotation of the C5-S bond in *cis*-2-terbutyl-5-tert-butylsulfenyl-1, 3-dioxane at M06-2X/6-311++G(2d,2p) level of theory.

X ray determination.

Details of data collection and processing of *cis*-1.

A block-shaped-shaped of *cis*-1 crystal with dimensions $0.21 \times 0.20 \times 0.19$ mm³ was mounted. Data were collected using a XtaLAB Synergy, Dualflex, HyPix diffractometer operating at $T = 99.99(10)$ K. Data were measured using *Mo K α* radiation. The diffraction pattern was indexed and the total number of runs and images was based on the strategy calculation from the program CrysAlisPro 1.171.41.98a (Rigaku OD, 2021). The maximum resolution that was achieved was $\Theta = 69.25^\circ$ (0.38 Å). The unit cell was refined using CrysAlisPro 1.171.41.98a (Rigaku OD, 2021) on 17577 reflections, 13% of the observed reflections. Data reduction, scaling and absorption corrections were performed using CrysAlisPro 1.171.41.98a (Rigaku OD, 2021). A gaussian absorption correction was performed using CrysAlisPro 1.171.41.98a (Rigaku Oxford Diffraction, 2021) Numerical absorption correction based on gaussian integration over a multifaceted crystal model Empirical absorption correction using spherical harmonics, implemented in SCALE3 ABSPACK scaling algorithm. The absorption coefficient μ of this material is 0.233 mm⁻¹ at this wavelength ($\lambda = 0.71073$ Å) and the minimum and maximum transmissions are 0.792 and 1.000. The structure was solved and the space group *Cc* (# 9) determined by the ShelXT (Sheldrick, 2015) structure solution program using iterative methods and refined by full matrix least squares minimisation on F^2 using version of olex2.refine 1.5 (Bourhis et al., 2015). In the initial independent atom model refinement, all non-hydrogen atoms were refined anisotropically. Hydrogen atom positions were calculated geometrically and refined using the riding model. A second refinement was performed using NoSpherA2, an implementation of NOn-SPHERical Atom-form-factors in Olex2.(Kleemiss F., 2021) NoSpherA2 implementation of HAR makes use of tailor-made aspherical atomic form factors calculated on-the-fly from a Hirshfeld-partitioned electron density (ED) - not from spherical-atom form factors. The ED is calculated from a gaussian basis set single determinant SCF wavefunction using wB97X DFT functional and def2-SVP basis set for a fragment of the crystal. This fragment is a cluster of 7 molecules, the central molecule and its 6 closest neighbors. For the calculation of the wavefunction Orca 4.2.1 (Neese, F. 2018) was used. The positions and the anisotropic displacement parameters (ADPs) of all atoms, H atoms included, were refined. Anharmonic parameter were refined solely for the S atom. A multipolar refinement was also performed using the XD2016 software (Volkov A. 2016). The initial atomic positions and ADPs were obtained from the Hirshfeld refinement. The R-H distances were fixed at the distance found in the Hirshfeld refinement. The spherical harmonics were used up to hexadecapoles for heavy atoms and up to dipoles for H atoms. The heavy atoms were refined anisotropically, while the H atoms isotropically. The anharmonic parameters of the S atom were also refined.

Table S1. Experimental details.

Refinament	Hirshfeld	Multipolar
Formula	C ₄₈ H ₉₆ O ₁₆ S ₄	
D _{calc.} / g cm ⁻³	1.253	
μ/mm ⁻¹	0.233	
Formula Weight	1057.552	
Shape	block-shaped	
Size/mm ³	0.21×0.20×0.19	
T/K	99.99(10)	
Crystal System	monoclinic	
Flack Parameter	0.025(8)	
Hooft Parameter	0.025(8)	
Space Group	Cc	
a/Å	22.8417(4)	
b/Å	5.94667(13)	
c/Å	10.39189(16)	
α/°	90	
β/°	96.6449(16)	
γ/°	90	
V/Å ³	1402.07(5)	
Z	1	
Z'	0.25	
Wavelength/Å	0.71073	
Radiation type	Mo K _α	
Θ _{min} /°	1.80	
Θ _{max} /°	69.25	
Measured Refl's.	136275	
R _{int}	0.0362	
Indep't Refl's	20798	
Refl's	16445 I≥2 σ(I)	17367 F≥3 σ(F)
Parameters	396	460
Largest Peak	0.2701	0.279
Deepest Hole	-0.2364	-0.296
GooF	1.0438	1.263
Refinament on	F ²	F
wR ₂	0.0375	0.0177
R ₁ (all data)	0.0368	0.0348
R ₁	0.0238	0.0255

Completeness Plot

unam-9-28-21_03

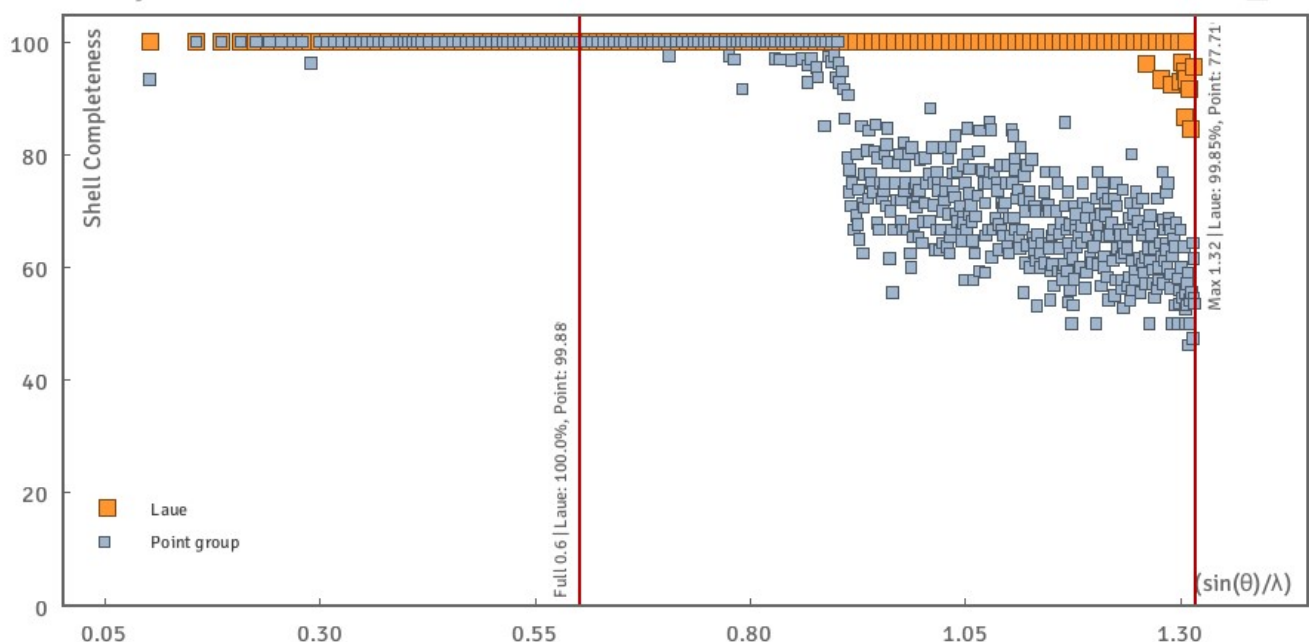


Figure S5. Data completeness.

Table S2. Quality of diffraction data.

$\sin \theta/\lambda$	I/σ	R_{merge}	$CC_{1/2}$
0.344	69.747	0.027	0.996
0.551	55.750	0.037	0.962
0.656	44.894	0.038	0.985
0.735	34.709	0.044	0.988
0.800	30.525	0.054	0.989
0.855	24.312	0.070	0.987
0.904	18.286	0.091	0.984
0.949	14.622	0.108	0.983
0.989	11.412	0.143	0.973
1.026	8.859	0.174	0.970
1.061	8.190	0.191	0.961
1.094	6.551	0.227	0.952
1.125	5.671	0.248	0.936
1.154	4.611	0.309	0.906
1.182	3.427	0.390	0.893
1.209	3.062	0.422	0.857
1.234	2.528	0.485	0.816
1.258	2.121	0.564	0.768
1.282	1.700	0.604	0.649
1.305	1.192	0.687	0.484

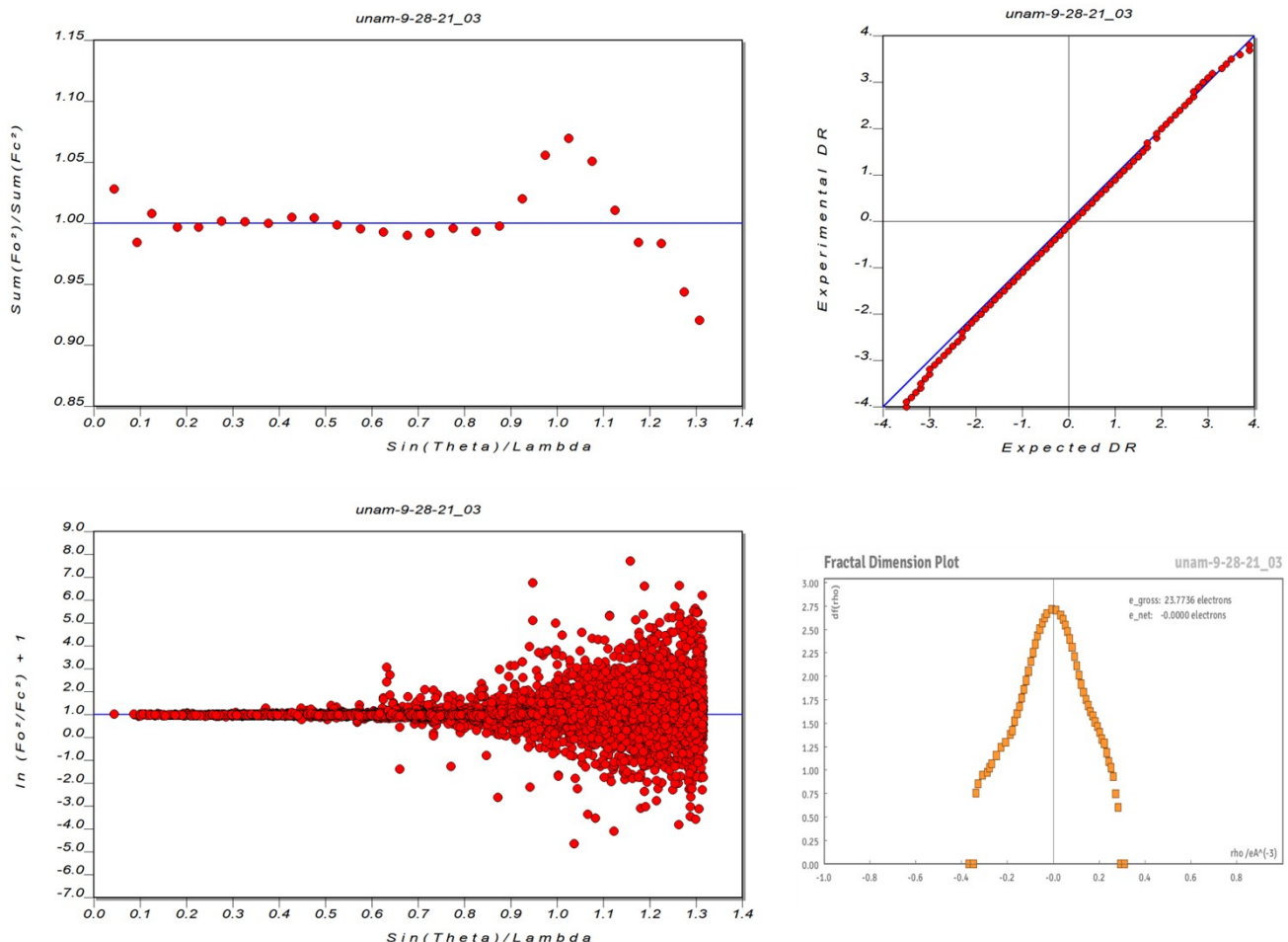


Figure S6. Plots from the Hirshfeld atom refinement of *cis*-1.

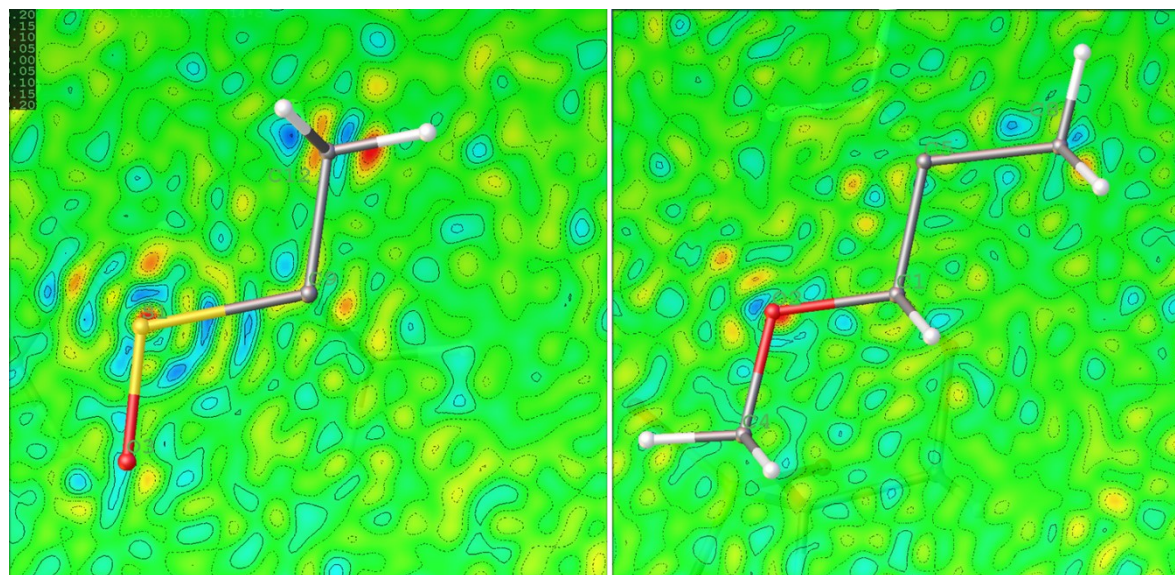


Figure S7. Residual density contour maps at $0.05 \text{ e}/\text{\AA}^3$ increments, after Hirshfeld refinement. On the left the $\text{O}(3)\text{S}(1)\text{C}(9)\text{C}(12)$ plane and on the right the $\text{C}(4)\text{O}(2)\text{C}(1)\text{C}(5)\text{C}(8)$ plane. Color code: $\geq 0.2 \text{ e}/\text{\AA}^3$ (blue), $0.0 \text{ e}/\text{\AA}^3$ (yellow) and $\leq -0.2 \text{ e}/\text{\AA}^3$ (red).

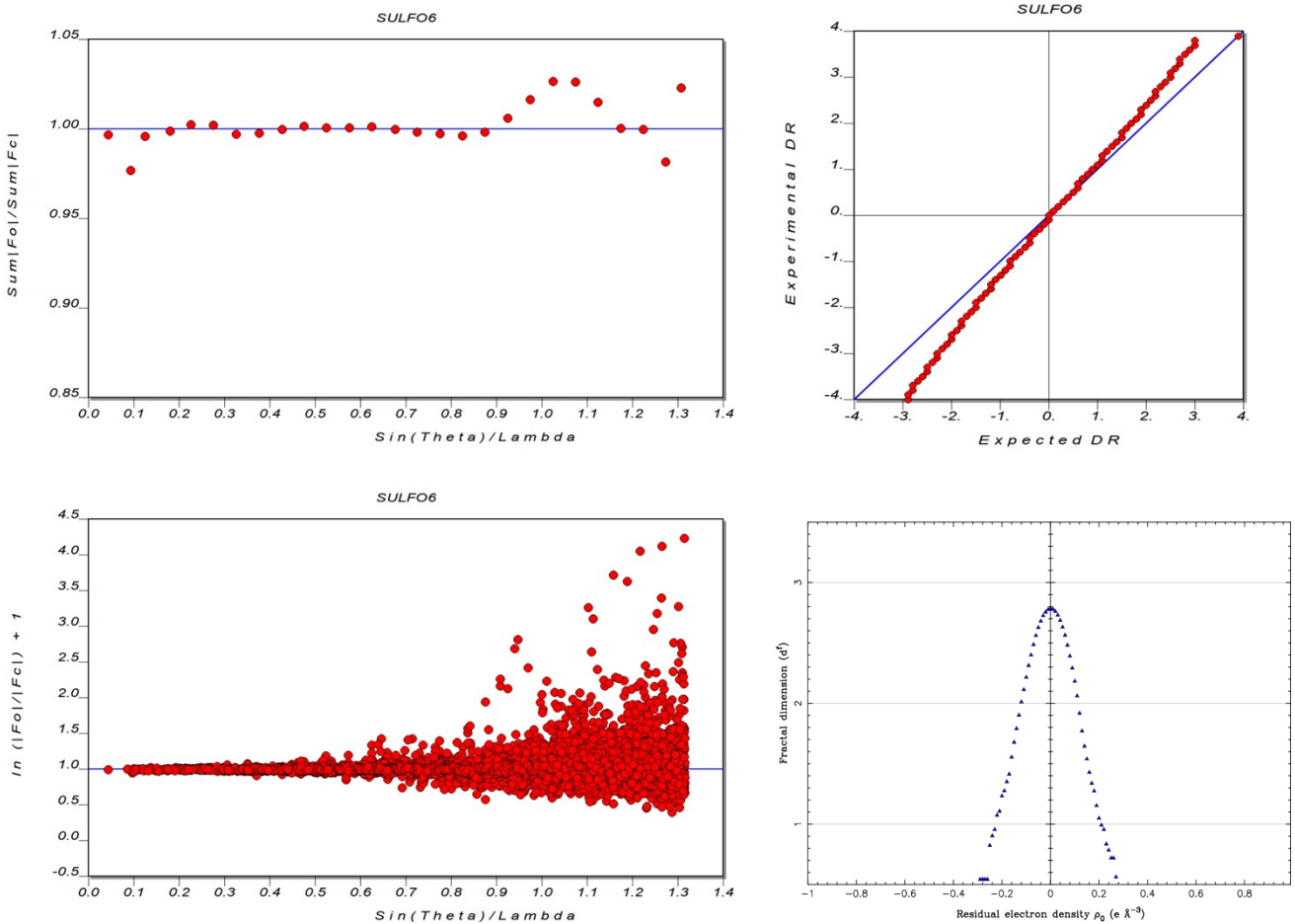


Figure S8. Plots from the Multipolar model refinement of *cis-1*.

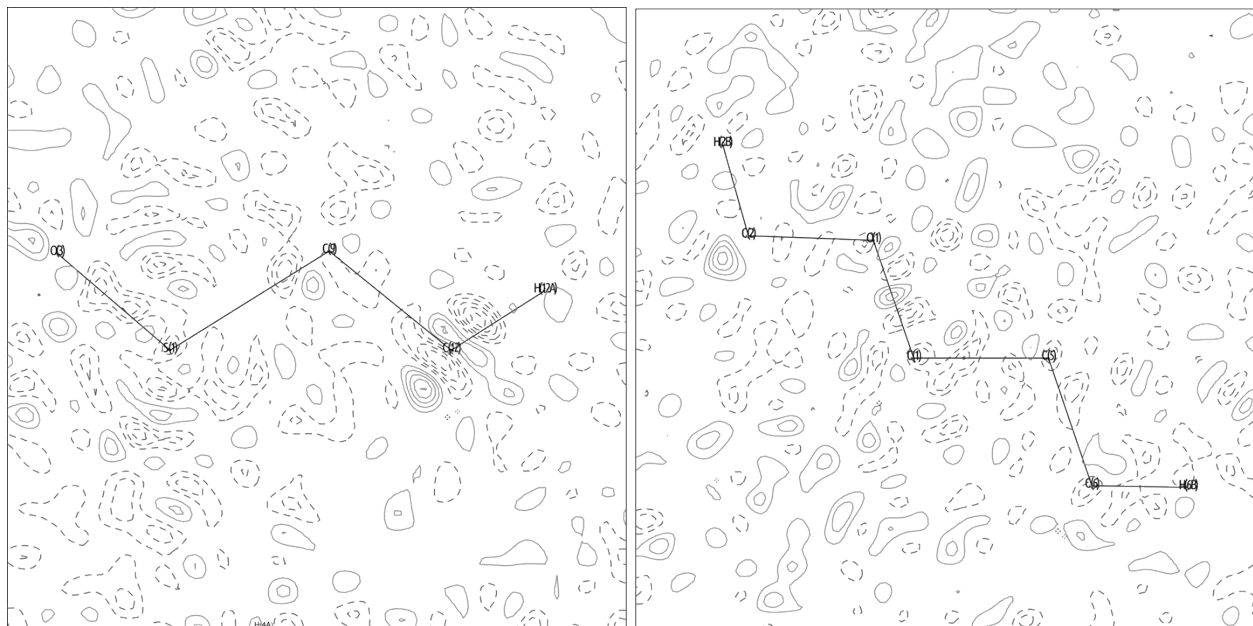


Figure S9. Residual density contour maps at $0.05 \text{ e}/\text{\AA}^3$ increments, after Multipolar refinement. On the left the $\text{O}(3)\text{S}(1)\text{C}(9)\text{C}(12)$ plane and on the right the $\text{C}(4)\text{O}(2)\text{C}(1)\text{C}(5)\text{C}(8)$ plane. Solid and dashed lines positive and negative values, respectively.

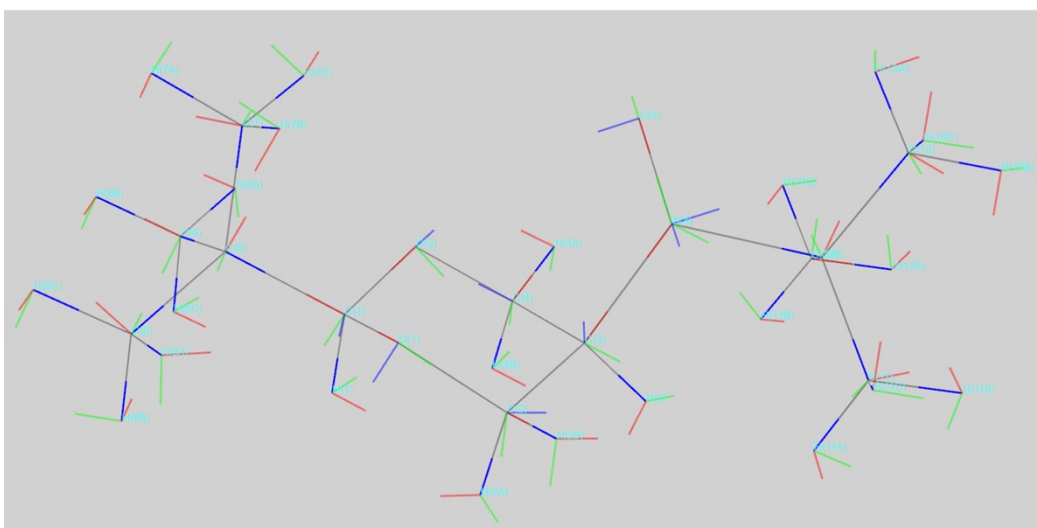
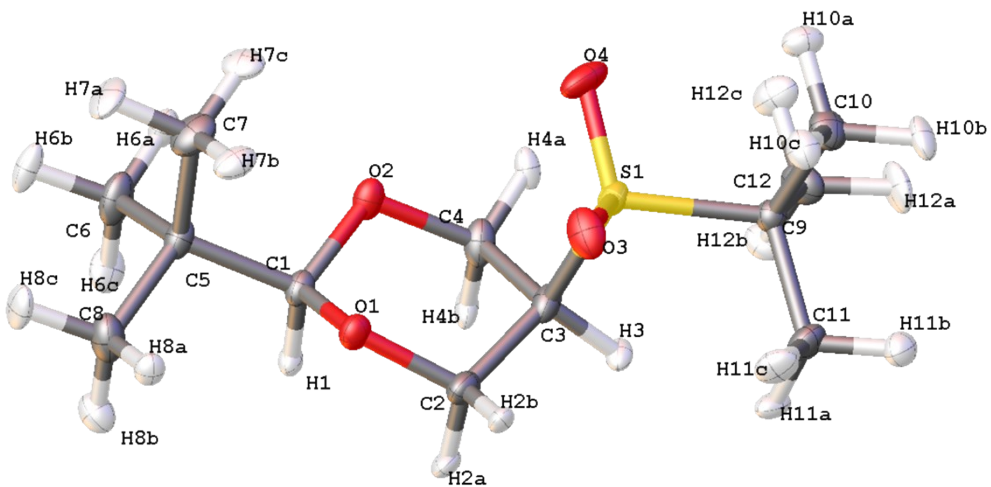


Figure S10. Atomic labels (top) and local coordinate system for the multipolar refinement (bottom). X (red), Y (green) and Z (blue) axis.

Topological theory of atoms in molecules section

Table S3. Density, laplacian, ellipticity and eigen values at the bond critical points (BCP). Values obtained after multipolar refinement.

	$\rho(\mathbf{r})/ e/\text{\AA}^3$	$\nabla^2\rho(\mathbf{r})/ e/\text{\AA}^5$	ε	λ_1	λ_2	λ_3
S(1)-O(3)	2.379	-14.328	0.011	-17.708	-17.520	20.899
O(4)-S(1)	2.269	-9.275	0.059	-15.064	-14.220	20.009
C(2)-H(2B)	1.994	-22.181	0.050	-19.897	-18.949	16.665
C(11)-H(11B)	1.968	-20.054	0.026	-17.274	-16.831	14.051
C(1)-O(2)	1.947	-17.625	0.084	-16.398	-15.134	13.907
C(1)-O(1)	1.946	-18.270	0.074	-16.590	-15.450	13.770
H(10A)-C(10)	1.946	-19.384	0.003	-17.138	-17.092	14.846
C(6)-H(6A)	1.946	-19.523	0.009	-17.697	-17.545	15.719
C(7)-H(7B)	1.934	-18.359	0.089	-17.646	-16.198	15.486
C(10)-H(10C)	1.929	-17.854	0.008	-16.572	-16.448	15.167
O(2)-C(4)	1.927	-12.143	0.123	-16.070	-14.316	18.243
H(12C)-C(12)	1.895	-16.466	0.192	-16.613	-13.936	14.082
C(7)-H(7C)	1.891	-18.667	0.086	-17.700	-16.294	15.327
C(10)-H(10B)	1.889	-17.814	0.004	-16.457	-16.389	15.032
O(1)-C(2)	1.882	-11.246	0.074	-14.901	-13.877	17.532
C(4)-H(4A)	1.874	-19.985	0.063	-19.111	-17.974	17.100
H(11A)-C(11)	1.873	-18.260	0.030	-16.554	-16.066	14.360
C(3)-H(3)	1.861	-17.315	0.075	-17.333	-16.130	16.148
H(4B)-C(4)	1.854	-15.734	0.043	-16.807	-16.117	17.190
H(8C)-C(8)	1.841	-16.171	0.024	-16.002	-15.631	15.462
C(11)-H(11C)	1.841	-17.685	0.027	-16.204	-15.771	14.290
H(6B)-C(6)	1.833	-17.743	0.007	-16.868	-16.753	15.877
H(12B)-C(12)	1.831	-14.742	0.190	-16.085	-13.512	14.856
H(8B)-C(8)	1.825	-16.780	0.022	-16.170	-15.816	15.206
H(1)-C(1)	1.810	-16.632	0.011	-17.020	-16.842	17.229
H(7A)-C(7)	1.805	-16.882	0.083	-16.968	-15.665	15.750
C(8)-H(8A)	1.775	-15.248	0.022	-15.522	-15.186	15.460
C(5)-C(1)	1.770	-13.322	0.069	-13.253	-12.396	12.327
H(2A)-C(2)	1.762	-15.124	0.025	-16.249	-15.848	16.973
C(12)-C(9)	1.752	-13.377	0.007	-12.687	-12.604	11.915
C(4)-C(3)	1.732	-13.280	0.021	-12.764	-12.502	11.986
C(12)-H(12A)	1.730	-13.600	0.176	-15.437	-13.126	14.963
H(6C)-C(6)	1.695	-16.420	0.009	-16.239	-16.093	15.912
C(9)-C(10)	1.690	-11.986	0.001	-11.961	-11.944	11.919
C(5)-C(7)	1.684	-11.239	0.027	-11.862	-11.548	12.171
C(8)-C(5)	1.679	-10.473	0.031	-11.674	-11.327	12.528
C(9)-C(11)	1.668	-10.444	0.006	-11.375	-11.309	12.239
C(6)-C(5)	1.636	-10.244	0.031	-11.369	-11.028	12.153
C(2)-C(3)	1.617	-10.866	0.073	-11.716	-10.917	11.766
S(1)-C(9)	1.284	-4.190	0.040	-8.021	-7.710	11.542
C(3)-S(1)	1.248	-4.384	0.086	-8.138	-7.495	11.249

Table S4. Density, laplacian, ellipticity and eigen values at the bond critical points (BCP) of intermolecular interactions. Values obtained after multipolar refinement.

	$\rho(\mathbf{r})/ e/\text{\AA}^3$	$\nabla^2\rho(\mathbf{r})/ e/\text{\AA}^5$	ε	$\lambda_{1\lambda}$	λ_2	λ_3
H(2B)-O(4)	0.079	1.245	0.075	-0.302	-0.281	1.827
H(3)-O(3)	0.070	1.346	0.058	-0.257	-0.243	1.846
O(1)-H(4B)	0.055	0.986	0.150	-0.180	-0.157	1.323
H(6A)-H(7A)	0.047	0.674	0.051	-0.161	-0.153	0.988
O(3)-H(12B)	0.043	0.748	0.166	-0.138	-0.119	1.006
O(3)-H(11A)	0.034	0.607	0.151	-0.100	-0.087	0.794
H(7C)-C(4)	0.033	0.395	0.518	-0.073	-0.048	0.515
C(12)-H(10A)	0.029	0.355	0.307	-0.054	-0.042	0.451
H(8A)-H(1)	0.027	0.411	0.146	-0.080	-0.070	0.561
H(12A)-H(8C)	0.026	0.442	0.109	-0.079	-0.071	0.593
H(11C)-H(10A)	0.025	0.429	0.229	-0.070	-0.057	0.555
O(2)-H(2A)	0.024	0.365	0.280	-0.061	-0.048	0.474
C(10)-H(6B)	0.024	0.297	1.027	-0.053	-0.026	0.376
C(10)-H(8B)	0.023	0.319	0.321	-0.055	-0.042	0.415
H(7B)-H(2A)	0.022	0.463	0.131	-0.064	-0.057	0.584
H(11B)-H(6C)	0.022	0.285	0.300	-0.051	-0.040	0.376
H(8A)-H(7C)	0.022	0.296	0.388	-0.052	-0.037	0.385
H(11A)-H(12C)	0.021	0.410	0.699	-0.066	-0.039	0.516
H(10B)-H(8C)	0.021	0.402	0.230	-0.061	-0.049	0.512
O(4)-H(11C)	0.017	0.255	0.333	-0.034	-0.025	0.313
O(4)-H(12B)	0.017	0.248	0.356	-0.037	-0.027	0.312
H(7B)-H(1)	0.017	0.265	0.766	-0.040	-0.023	0.328
H(6A)-H(8B)	0.016	0.237	0.194	-0.037	-0.031	0.305
H(6C)-H(8A)	0.014	0.200	1.332	-0.031	-0.013	0.245
H(12A)-H(6B)	0.014	0.274	0.356	-0.036	-0.027	0.337

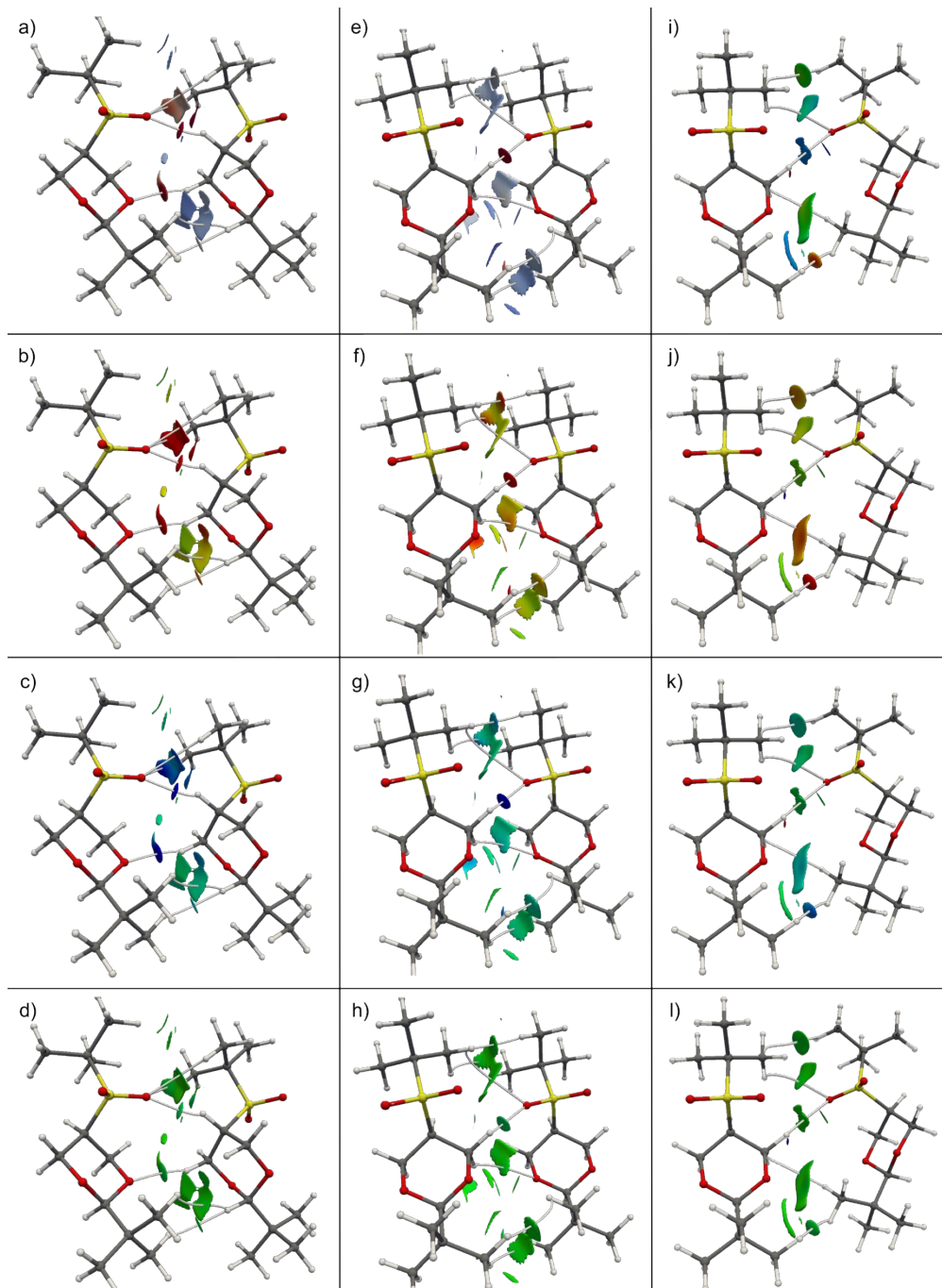


Figure S11. Intermolecular 0.5 RDG isosurface of *cis*-1 pairs A (left) , B (center) and C (right). The isosurfaces are colored by $\rho(\mathbf{r})$ (top), $\nabla^2\rho(\mathbf{r})$ (second top), $K(\mathbf{r})$ (second bottom) and $\text{sign}\lambda_2\rho$ (NCI, bottom) scalar fields. $\rho(\mathbf{r})$ color code: $\geq 5.0 \times 10^{-2} \text{ e}/\text{\AA}^3$ (red), $2.5 \times 10^{-2} \text{ e}/\text{\AA}^3$ (green) and $0.0 \text{ e}/\text{\AA}^3$ (dark blue). $\nabla^2\rho(\mathbf{r})$ color code: $\leq -5.0 \times 10^{-1} \text{ e}/\text{\AA}^5$ (dark blue), $0.0 \text{ e}/\text{\AA}^5$ (green) and $\geq 5.0 \times 10^{-1} \text{ e}/\text{\AA}^5$ (red). $K(\mathbf{r})$ color code: $\leq -5.0 \times 10^{-2} \text{ e}/\text{\AA}^5$ (dark blue), $0.0 \text{ e}/\text{\AA}^5$ (green) and $\geq 5.0 \times 10^{-2} \text{ e}/\text{\AA}^5$ (red). $\text{sign}\lambda_2\rho$ color code: $\leq -5.0 \times 10^{-2} \text{ a.u.}$ (dark blue), 0.0 a.u. (green) and $\geq 5.0 \times 10^{-2} \text{ a.u.}$ (red).

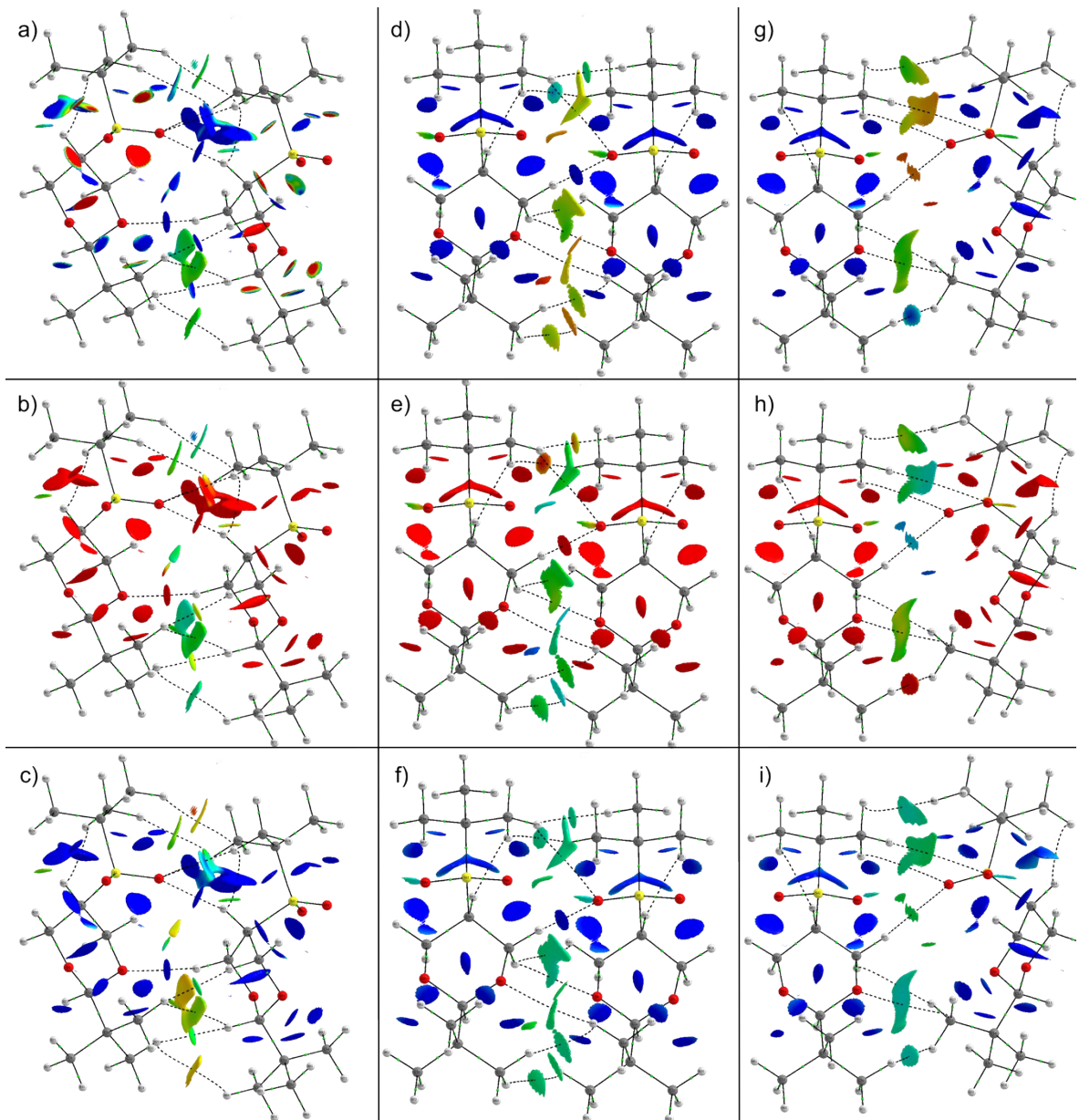


Figure S12. Theoretical (ω -B97XD/Def2-TZVP) 0.5 RDG isosurface of *cis*-1 pairs A (left), B (center) and C (right). The isosurfaces are colored by $V(\mathbf{r})$ (top), $G(\mathbf{r})$ (center) and $G(\mathbf{r})$ (bottom) scalar fields. $V(\mathbf{r})$ color code: $\leq -1.0 \times 10^{-1} \text{ e}/\text{\AA}^5$ (dark blue), $-5.0 \times 10^{-2} \text{ e}/\text{\AA}^5$ (green) and $0.0 \text{ e}/\text{\AA}^5$ (red). $K(\mathbf{r})$ color code: $\leq -5.0 \times 10^{-2} \text{ e}/\text{\AA}^5$ (dark blue), $0.0 \text{ e}/\text{\AA}^5$ (green) and $\geq 5.0 \times 10^{-2} \text{ e}/\text{\AA}^5$ (red). $G(\mathbf{r})$ color code: $\geq 1.0 \times 10^{-1} \text{ e}/\text{\AA}^5$ (red), $5.0 \times 10^{-2} \text{ e}/\text{\AA}^5$ (green) and $0.0 \text{ e}/\text{\AA}^5$ (dark blue).

Thermochemistry section

Enthalpies of sublimation by thermogravimetry

The sublimation enthalpy of each dioxane were measured by thermogravimetric analysis (TGA) and applying the Langmuir equation¹, which relates the mass loss of a sample with its vapour pressure during the sublimation process:

$$(dm/dt)(1/A) = p\gamma\sqrt{M/2\pi RT}. \quad (1)$$

In this equation (dm/dt) is the rate of mass loss at the temperature T for a sample with a sublimation area A ; p is the vapour pressure; M is the molar mass; R is the gas constant and γ is the constant of vaporisation. If the enthalpy of sublimation, $\Delta_{\text{sub}}H_{\text{m}}(T)$, is the quantity to be measured and the vapour pressures are not required, the direct combination of the Langmuir equation with the known Clausius-Clapeyron equation leads to the following expression:

$$\ln[(1/A)\cdot(dm/dt)\cdot(T/M)^{1/2}] = \ln B - \Delta_{\text{sub}}H_{\text{m}}(T)/RT, \quad (2)$$

where dm/dt is the rate of loss of mass at the temperature T and B is a constant which includes all other constant terms from the combined equations. The factor $(1/A)\cdot(dm/dt)\cdot(T/M)^{1/2}$ is usually denoted as upsilon υ . Then, a graphic $\ln \upsilon$ vs. $1/T$ is linear and its slope is the enthalpy of sublimation. The reliability of this methodology for deriving accurate results of sublimation enthalpy has already been shown^{2,3}.

For the application of equation (2), the rate of mass loss as a function of temperature was determined from the thermogravimetric curve obtained by using a TA Instruments SDT Q600. The sensitive element in this instrument is a dual-beam thermobalance with a 200-mg sample capacity and 0.1 μg sensitivity. A thermocouple in each beam measures the temperature of the samples located on it with an uncertainty of ± 0.01 $^{\circ}\text{C}$, and the beams operate inside of a furnace with a temperature control of ± 1.0 $^{\circ}\text{C}$. The heating rate and the flow of the purge gas in the furnace can be controlled with a sensitivity of 0.1 $^{\circ}\text{C}\cdot\text{min}^{-1}$ and 1.0 $\text{cm}^3\cdot\text{min}^{-1}$ respectively. The TGA/DSC device was calibrated for mass measurement with a standard mass traceable to NIST of (315.1620 ± 0.0048) mg. The temperature scale was calibrated by analysing the melting temperature of NIST 2232 Indium.

Preliminary experiments to establish the best sublimation conditions showed that masses of 2.0 to 2.5 mg uniformly distributed in the bottom of a 5.5 mm diameter alumina cup located on the

beam of the thermobalance, were sufficient to generate continuous and smooth thermogravimetric curves (See the Supporting information). These preliminary tests also set up an interval of temperature from 30.0 to 250.0 °C as optimal for the scanning in temperature, with a heating rate of 10.0 °C·min⁻¹ and under a nitrogen flow of 100.0 mL·min⁻¹, in order to reach total vaporisation of each dioxane.

Once the sample was located in the measurement beam of the thermogravimetric device, its temperature was equilibrated at 30.0 °C and after a couple of minutes the scanning for temperature and data acquisition were started. The mass loss rate (dm/dt) to substitute in equation (2), was computed from data of the respective derivative curve (See Supporting Information), which was generated using the *Universal Analysis* software of the SDT Q600 device. A set of four to six series utilizing this methodology were performed on each dioxane studied in this research.

Determination of Enthalpies of Fusion.

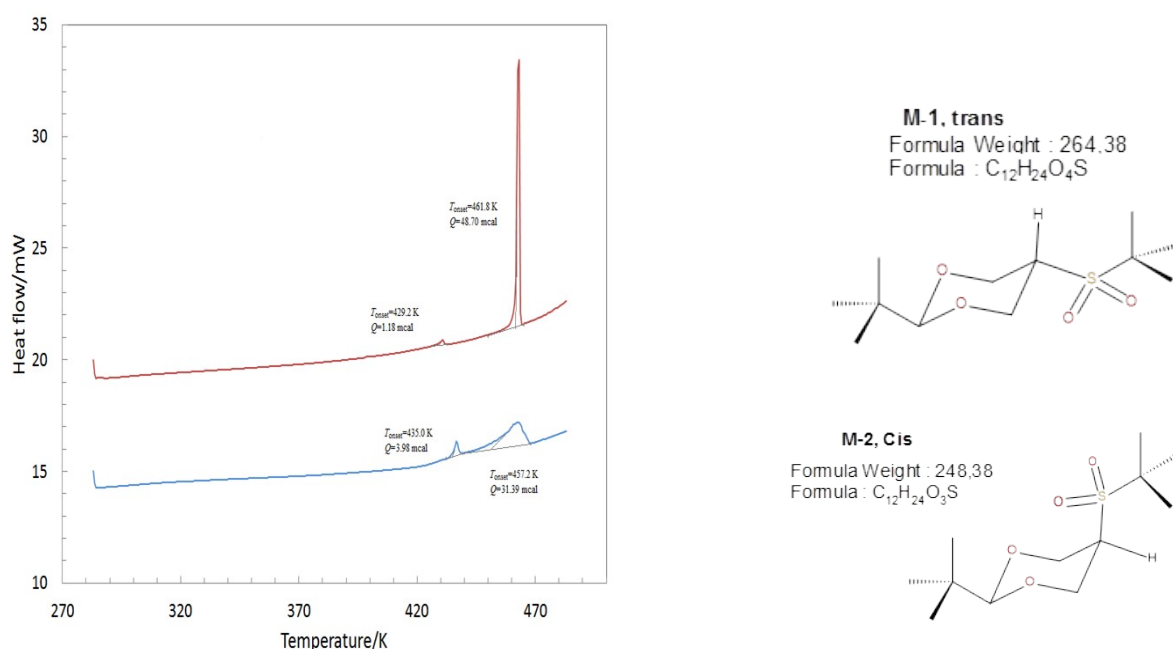


Table S5.^a DSC results of crystalline transition and fusion, temperatures and enthalpies, for the dioxanes.

Figure S13. Representative DSC heat flux as a function of the temperature curves for the dioxanes. Trans isomer in red; cis isomer in blue. Note the crystalline transition prior to the fusion for both dioxanes.

m_{sample}	T_{tr}	\mathcal{Q}_{tr}	$\Delta_{\text{tr}}H_m(T_{\text{tr}})$	purity	T_{fus}	\mathcal{Q}_{fus}	$\Delta_{\text{fus}}H_m(T_{\text{fus}})$
mg	K	mcal	kcal · mol ⁻¹	mole fraction	K	mcal	kcal · mol ⁻¹
<i>trans</i> isomer							
1.972	429.2	1.18	0.16	0.9999	461.8	48.70	6.53
2.072	429.8	1.13	0.15	0.9984	462.0	52.67	6.87
1.871	429.4	1.15	0.16	0.9816	459.4	47.93	6.77
	429.5 ± 0.3		0.16 ± 0.01	0.9933 ± 0.010	461.1 ± 1.2		6.72 ± 0.18
<i>cis</i> isomer							
2.119	435.4	3.95	0.49	0.9450	454.5	34.65	4.32
1.990	435.0	3.98	0.53	0.9499	457.2	31.39	4.17
	435.2 ± 0.3		0.51 ± 0.03	0.9475 ± 0.003	455.8 ± 1.5		4.25 ± 0.11

^aUncertainty associated to each average value was calculated as the standard deviation.

Determination of Enthalpies of Sublimation

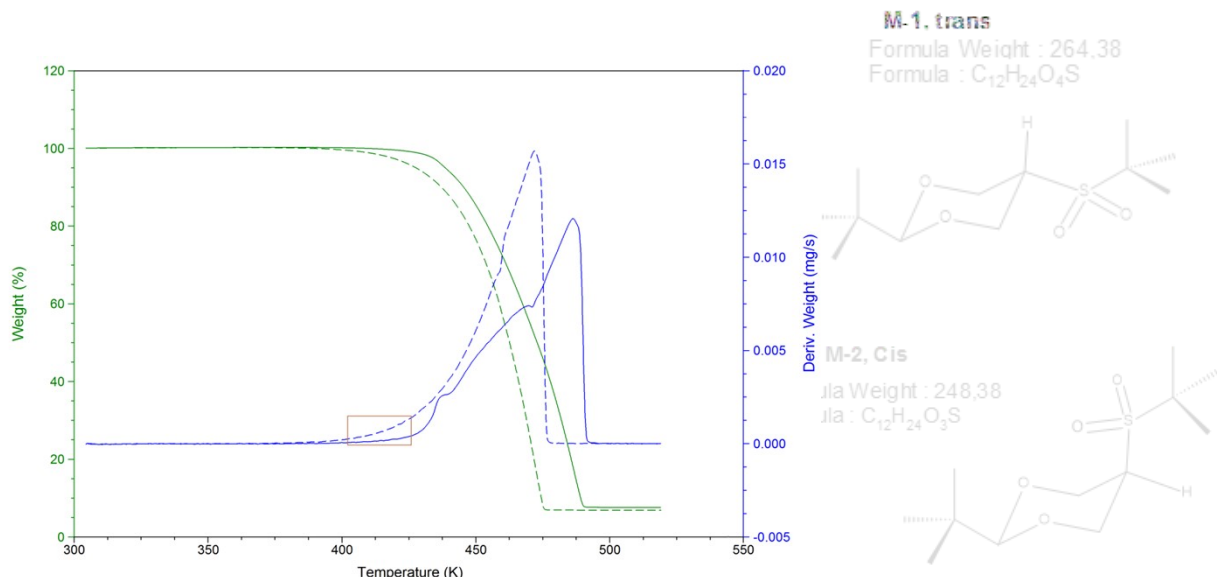


Figure S14. Representative thermogravimetric (in green) and derivative in time dm/dt (in blue) curves, as a function of the temperature T , for the change of phase of the dioxanes; --- *trans* isomer; — *cis* isomer. The brown frame indicates the mass loss rate for the solid compounds in the range of temperature where data to calculate the enthalpies of sublimation were measured.

Table S6^a

Experimental data of the dependence of the loss mass rate with the temperature and the enthalpies of sublimation derived from the thermogravimetric experiments of the ***trans*** isomer. The term ν is defined as $(1/A)(dm/dt)(T/M)^{1/2}$.

T/K	m/mg	(dm/dt)·10 ¹⁰		$\nu \cdot 10^4$ $(\text{kg} \cdot \text{K} \cdot \text{mol})^{1/2} \cdot \text{s}^{-1}$	10^3 T	ln ν
		kg·s ⁻¹	(kg · K · mol) ^{1/2} · s ⁻¹			
Series 1						
404.0	1.9729	3.005	3.652	2.475	-7.915	
406.0	1.9690	3.648	4.444	2.463	-7.719	
408.0	1.9644	4.044	4.938	2.451	-7.613	
410.0	1.9595	4.257	5.211	2.439	-7.560	
412.0	1.9537	4.852	5.954	2.427	-7.426	
414.0	1.9468	6.550	8.057	2.415	-7.124	
416.0	1.9380	7.841	9.668	2.404	-6.941	
418.0	1.9283	8.463	10.460	2.392	-6.863	
420.0	1.9170	10.352	12.826	2.381	-6.659	
422.0	1.9039	11.699	14.529	2.370	-6.534	
424.0	1.8891	13.044	16.238	2.358	-6.423	
$\ln \nu = -13187.7/T + 24.7; \quad r^2 = 0.9869; \quad \sigma_a = 1.2; \quad \sigma_b = 505.6; \quad \Delta_{\text{sub}}H_m(414 \text{ K})/\text{kcal} \cdot \text{mol}^{-1} = 26.2 \pm 1.0$						
Series 2:						
404.0	2.0350	3.193	3.880	2.475	-7.855	
406.0	2.0310	3.648	4.444	2.463	-7.719	
408.0	2.0261	4.331	5.289	2.451	-7.545	
410.0	2.0207	4.919	6.021	2.439	-7.415	
412.0	2.0144	5.743	7.047	2.427	-7.258	
414.0	2.0070	6.609	8.130	2.415	-7.115	
416.0	1.9984	7.626	9.403	2.404	-6.969	
418.0	1.9884	8.862	10.953	2.392	-6.817	
420.0	1.9770	10.210	12.650	2.381	-6.673	
422.0	1.9638	11.739	14.579	2.370	-6.531	
424.0	1.9486	13.411	16.695	2.358	-6.395	
$\ln \nu = -12576.1/T + 23.3; \quad r^2 = 0.9998; \quad \sigma_a = 0.16; \quad \sigma_b = 65.2; \quad \Delta_{\text{sub}}H_m(414 \text{ K})/\text{kcal} \cdot \text{mol}^{-1} = 25.0 \pm 0.1$						
Series 3						
404.0	2.7140	3.044	3.699	2.475	-7.902	
406.0	2.7100	3.762	4.583	2.463	-7.688	
408.0	2.7050	4.187	5.113	2.451	-7.579	
410.0	2.6990	4.938	6.045	2.439	-7.411	
412.0	2.6930	5.780	7.093	2.427	-7.251	
414.0	2.6860	6.687	8.226	2.415	-7.103	
416.0	2.6770	7.451	9.187	2.404	-6.993	
418.0	2.6670	8.855	10.945	2.392	-6.817	
420.0	2.6560	10.300	12.761	2.381	-6.664	
422.0	2.6420	11.580	14.381	2.370	-6.544	
424.0	2.6270	13.650	16.992	2.358	-6.378	
$\ln \nu = -12763.0/T + 23.7; \quad r^2 = 0.9987; \quad \sigma_a = 0.39; \quad \sigma_b = 161.4; \quad \Delta_{\text{sub}}H_m(414 \text{ K})/\text{kcal} \cdot \text{mol}^{-1} = 25.4 \pm 0.3$						
Series 4						
404.0	2.0362	3.336	4.053	2.475	-7.811	
406.0	2.0318	3.978	4.846	2.463	-7.632	
408.0	2.0267	4.664	5.695	2.451	-7.471	
410.0	2.0206	5.434	6.652	2.439	-7.315	
412.0	2.0137	6.075	7.455	2.427	-7.202	
414.0	2.0057	7.161	8.809	2.415	-7.035	
416.0	1.9964	8.443	10.411	2.404	-6.868	
418.0	1.9856	9.579	11.840	2.392	-6.739	
420.0	1.9734	10.823	13.409	2.381	-6.614	
422.0	1.9591	12.827	15.930	2.370	-6.442	
424.0	1.9416	15.260	18.996	2.358	-6.266	
$\ln \nu = -12878.7/T + 24.1; \quad r^2 = 0.9987; \quad \sigma_a = 0.37; \quad \sigma_b = 154.4; \quad \Delta_{\text{sub}}H_m(414 \text{ K})/\text{kcal} \cdot \text{mol}^{-1} = 25.6 \pm 0.3$						
Series 5						

404.0	2.5508	3.638	4.421	2.475	-7.724			
406.0	2.5461	4.171	5.081	2.463	-7.585			
408.0	2.5406	4.721	5.765	2.451	-7.459			
410.0	2.5343	5.772	7.066	2.439	-7.255			
412.0	2.5270	6.518	7.998	2.427	-7.131			
414.0	2.5186	7.639	9.397	2.415	-6.970			
416.0	2.5086	8.786	10.834	2.404	-6.828			
418.0	2.4971	10.113	12.500	2.392	-6.685			
420.0	2.4840	11.729	14.532	2.381	-6.534			
422.0	2.4689	13.391	16.630	2.370	-6.399			
424.0	2.4518	15.298	19.044	2.358	-6.264			
$\ln \upsilon = -12665.5/T + 23.6; r^2 = 0.9993; \sigma_a = 0.43; \sigma_b = 179.0;$			$\Delta_{sub}H_m(414 \text{ K})/\text{kcal}\cdot\text{mol}^{-1} = 25.2 \pm 0.4$					
Series 6								
404.0	2.1095	3.118	3.789	2.475	-7.878			
406.0	2.1053	3.869	4.713	2.463	-7.660			
408.0	2.1004	4.281	5.228	2.451	-7.556			
410.0	2.0948	5.027	6.154	2.439	-7.393			
412.0	2.0883	5.878	7.213	2.427	-7.234			
414.0	2.0808	6.690	8.229	2.415	-7.103			
416.0	2.0721	7.801	9.619	2.404	-6.947			
418.0	2.0620	9.059	11.197	2.392	-6.795			
420.0	2.0504	10.407	12.894	2.381	-6.654			
422.0	2.0370	11.860	14.729	2.370	-6.521			
424.0	2.0215	13.697	17.051	2.358	-6.374			
$\ln \upsilon = -12672.9/T + 23.5; r^2 = 0.9990; \sigma_a = 0.34; \sigma_b = 138.7;$			$\Delta_{sub}H_m(414 \text{ K})/\text{kcal}\cdot\text{mol}^{-1} = 25.2 \pm 0.3$					
Weighted average value: $\langle \Delta_{sub}H_m(\text{trans isomer}, 414 \text{ K}) \rangle/\text{kcal}\cdot\text{mol}^{-1} = 25.1 \pm 0.1$								
$\Delta_{sub}H_m(\text{trans isomer}, 298.15 \text{ K})/\text{kcal}\cdot\text{mol}^{-1} = 26.0 \pm 0.1$								
^a $\upsilon = (1/A)(dm/dt)(T/M)^{1/2}$, where $A = 1.662 \times 10^{-5} \text{ m}^2$ calculated from sample cup diameter and the molar mass $M = 264.383 \text{ g}\cdot\text{mol}^{-1}$ computed from the 2011 IUPAC Atomic Masses ⁴ . Parameters σ_a and σ_b represent the standard deviation of the intercept and slope of the function $\ln \upsilon$ vs $1/T$. Uncertainty for each sublimation enthalpy value was computed as $\sigma_b \cdot R$. The weighted average value μ and its standard deviation σ , were calculated as $\mu = \sum(x_i/\sigma_i^2)/\sum(1/\sigma_i^2)$ and $\sigma^2 = [1/\sum(1/\sigma_i^2)]$, where x_i is each of the N sublimation enthalpy data and its respective standard deviation σ_i ⁵ . Enthalpy of sublimation at 298.15 K was computed from the experimental weighted average value by applying the equation $\Delta_{sub}H_m(298.15 \text{ K}) = \Delta_{sub}H_m(T_{exp}) + [0.07648 \text{ kcal K}^{-1}\text{mol}^{-1}(T_{exp} - 298.15 \text{ K})]$, suggested by Chickos <i>et al</i> ⁶ .								

Table S7^a

Experimental data of the dependence of the loss mass rate with the temperature and the enthalpies of sublimation derived from the thermogravimetric experiments of the **cis isomer**. The term ν is defined as $(1/A)(dm/dt)(T/M)^{1/2}$.

T/K	m/mg	(dm/dt) · 10 ¹⁰		$\nu \cdot 10^4$ (kg · K · mol) ^{1/2} · s	10 ³ T	ln ν
		kg · s ⁻¹	<i>cis</i> isomer			
Series 1						
414.0	2.2869	1.406		1.729	2.415	-8.663
416.0	2.2847	1.441		1.777	2.404	-8.636
418.0	2.2831	2.009		2.483	2.392	-8.301
420.0	2.2804	2.879		3.567	2.381	-7.939
422.0	2.2767	3.332		4.138	2.370	-7.790
424.0	2.2729	3.096		3.854	2.358	-7.861
426.0	2.2686	3.875		4.835	2.347	-7.634
428.0	2.2633	4.855		6.072	2.336	-7.407
430.0	2.2567	6.370		7.986	2.326	-7.133
$\ln \nu = -16645.1/T + 31.5; r^2 = 0.9566; \sigma_a = 3.17; \sigma_b = 1339.5; \Delta_{sub}H_m(422 \text{ K})/\text{kcal} \cdot \text{mol}^{-1} = 33.1 \pm 2.7$						
Series 2:						
414.0	2.1398	1.637		2.014	2.415	-8.510
416.0	2.1379	1.744		2.150	2.404	-8.445
418.0	2.1356	2.025		2.503	2.392	-8.293
420.0	2.1330	2.318		2.872	2.381	-8.155
422.0	2.1299	2.677		3.325	2.370	-8.009
424.0	2.1263	3.288		4.093	2.358	-7.801
426.0	2.1220	4.082		5.093	2.347	-7.582
428.0	2.1162	5.592		6.994	2.336	-7.265
430.0	2.1085	7.558		9.475	2.326	-6.962
$\ln \nu = -17036.4/T + 32.5; r^2 = 0.9581; \sigma_a = 3.25; \sigma_b = 1372.4; \Delta_{sub}H_m(422 \text{ K})/\text{kcal} \cdot \text{mol}^{-1} = 33.9 \pm 2.7$						
Series 3						
414.0	2.4440	1.604		1.973	2.415	-8.531
416.0	2.4420	1.631		2.011	2.404	-8.512
418.0	2.4398	2.077		2.567	2.392	-8.268
420.0	2.4369	2.419		2.997	2.381	-8.113
422.0	2.4339	2.769		3.439	2.370	-7.975
424.0	2.4302	3.413		4.249	2.358	-7.764
426.0	2.4257	4.130		5.153	2.347	-7.571
428.0	2.4200	5.285		6.610	2.336	-7.322
430.0	2.4125	7.182		9.003	2.326	-7.013
$\ln \nu = -16865.0/T + 32.1; r^2 = 0.9761; \sigma_a = 2.51; \sigma_b = 1057.5; \Delta_{sub}H_m(422 \text{ K})/\text{kcal} \cdot \text{mol}^{-1} = 33.5 \pm 2.1$						
Series 4						
414.0	2.3098	1.744		2.145	2.415	-8.447
416.0	2.3078	1.840		2.269	2.404	-8.391
418.0	2.3054	2.131		2.634	2.392	-8.242
420.0	2.3026	2.507		3.106	2.381	-8.077
422.0	2.2993	3.045		3.782	2.370	-7.880
424.0	2.2955	3.503		4.361	2.358	-7.738
426.0	2.2907	4.224		5.271	2.347	-7.548
428.0	2.2848	5.593		6.995	2.336	-7.265
430.0	2.2768	8.002		10.031	2.326	-6.905
$\ln \nu = -16694.0/T + 31.7; r^2 = 0.9627; \sigma_a = 2.94; \sigma_b = 1241.8; \Delta_{sub}H_m(422 \text{ K})/\text{kcal} \cdot \text{mol}^{-1} = 33.2 \pm 2.5$						
Weighted average value: $<\Delta_{sub}H_m(\text{cis isomer}, 422 \text{ K})>/\text{kcal} \cdot \text{mol}^{-1} = 33.4 \pm 1.2$						
$\Delta_{sub}H_m(\text{cis isomer}, 298.15 \text{ K})/\text{kcal} \cdot \text{mol}^{-1} = 34.4 \pm 1.2$						

^a $\nu = (1/A)(dm/dt)(T/M)^{1/2}$, where $A = 1.662 \times 10^{-5} \text{ m}^2$ calculated from sample cup diameter and the molar mass $M=264.383 \text{ g mol}^{-1}$ computed from the 2011 IUPAC Atomic Masses⁴. Parameters σ_a and σ_b represent the standard deviation of the

intercept and slope of the function $\ln v$ vs $1/T$. Uncertainty for each sublimation enthalpy value was computed as $\sigma_b \cdot R$. The weighted average value μ and its standard deviation σ , were calculated as $\mu = \sum(x_i/\sigma_i^2)/\sum(1/\sigma_i^2)$ and $\sigma^2 = [1/\sum(1/\sigma_i^2)]$, where x_i is each of the N sublimation enthalpy data and its respective standard deviation σ_i^2 . Enthalpy of sublimation at 298.15 K was computed from the experimental weighted average value by applying the equation $\Delta_{sub}H_m(298.15\text{ K}) = \Delta_{sub}H_m(T_{exp}) + [0.07648\text{ kcal K}^{-1}\text{mol}^{-1} \cdot (T_{exp} - 298.15\text{ K})]$, suggested by Chickos *et al*⁶.

References

1. Langmuir, I. The vapor pressure of metallic tungsten, *Phys. Rev.*, 1913, **2**, 329-342.
2. Sánchez-Bulás, T; Cruz-Vásquez, O; Hernández-Obregón, J; Rojas, A., *Thermochim. Acta.*, 2016 In press.
3. Melchor Martínez Herrera, Myriam Campos, Luis Alfonso Torres, Aarón Rojas, Enthalpies of Sublimation of Fullerenes by Thermogravimetry, *Thermochim Acta*. 622 (2015) 72-81.
4. Wieser, M. E.; Holden, N.; Coplen, T. B.; Böhlke, J. K.; Berglund, M.; Brand, W. A.; De Bièvre, P.; Gröning, M.; Loss, R. D.; Meija, J.; Hirata, T.; Prohaska, T.; Schoenberg, R.; O'Connor, G.; Walczyk, T.; Yoneda, S.; Zhu, X. K. Atomic weights of the elements 2011 (IUPAC technical report), *Pure Appl. Chem.* 85 (2013) 1047–1078.
5. Bevington, P. R.; Robinson, D. K.; Data reduction and error analysis for the Physical Sciences, 3rd edition, McGraw-Hill Higher Education, New York, 2003.
6. Chickos, J. S.; Hosseini, S.; Hesse, D. G.; Liebman, J. F.; Heat capacity corrections to the standard state: A comparison of new and some literature methods for organic liquids and solids, *Struct. Chem.* 4 (1993) 271-278.